Hindawi
Shock and Vibration
Volume 2023, Article ID 4508247, 8 pages
https://doi.org/10.1155/2023/4508247

Research Article

A Method for Enhancing the Acoustic Scattering Characteristics of Underwater Acoustic Corner Reflectors in Vacuum Cavities

Jingzhuo Zhang, Dawei Xiao, and Taotao Xie

Naval University of Engineering, Wuhan 40033, China

Correspondence should be addressed to Dawei Xiao; david_engineer@126.com

Received 16 May 2023; Revised 23 October 2023; Accepted 25 October 2023; Published 6 November 2023

Academic Editor: Chao Tao

To alleviate the problem of unsatisfactory target strength and scattering stability of an underwater corner reflector, a method to enhance the acoustic scattering characteristics using a vacuum cavity as an acoustic reflecting layer is proposed. According to the principle of acoustic impedance mismatch of a water-reflecting layer, a vacuum cavity corner reflector is designed to take advantage of the property that sound waves cannot propagate under vacuum conditions. The acoustic vacuum reflecting layer has a theoretical acoustic reflecting coefficient of one. Comparative analyses are carried out with the single-layer metal corner reflector in terms of frequency and angle of incidence. For the concave structure of the underwater corner reflector, the structural finite element software ANSYS combined with the acoustic analysis software SYSNOISE is used to simulate and analyse the acoustic scattering characteristics, and the consistency of the simulation calculations and experimental data is verified through the pool experiments for typical cases. The results show that under the same reflection area, the vacuum cavity underwater corner reflector has large scattering intensity, good antiacoustic performance, no obvious frequency characteristics, and good decoupling effects. The target echo intensity value can be increased by 2 dB for better scattering stability. The overall weight is reduced by about 20 kg, with considerable engineering practicality, proving that the true cavity corner reflector is an ideal underwater acoustic counter-acoustic device.

1. Introduction

As a passive signal reflecting device, the corner reflector was first applied in the field of electromagnetic wave confrontation [1–4]. The device has the advantages of strong echo signals, low manufacturing cost, and simple processing [5]. In contrast to radar electromagnetic wave confrontation, the use of corner reflectors to simulate the acoustic reflection characteristics of underwater targets and to construct acoustic decoys is a new technological way to decoy active sonar and underwater weaponry.

The underwater corner reflector is a concave structure, so the underwater acoustic wave reflection process is more complex. In addition to the secondary waves caused by the vibrations reflected from the elastic structure, geometric and elastic scattering waves will also be scattered from the other reflecting surfaces many times, resulting in a variety of scattering waves that interact with each other [6]. The complex process of backward reflection of waves is collectively referred to as the scattering wave.

Scattered waves can be detected and received at any measurement point in space, which can be used to detect and locate underwater targets. Using the excellent acoustic echo characteristics of the underwater corner reflector and by simulating the underwater target sonar reflection echo, the combination of multiple underwater corner reflectors can be used to mark the underwater structure and simulate the underwater dummy target, so as to realise the simulation of the underwater target echo intensity value and scale characteristics [7].

The calculation methods for determining the acoustic scattering characteristics of underwater targets are divided into analytical and numerical analysis methods [8]. For the acoustic scattering calculation of complex structures, the

numerical method is usually used. For complex target shapes, the finite element solution method [9] is used, but its computational volume is large, and it cannot accurately solve the infinite-domain acoustic scattering problem. The boundary element method [10] applies to any complex target shape and can solve the infinite-domain scattering acoustic field problem, but it is difficult to calculate the high-frequency scattering of large-scale targets. Therefore, for such small and complex structural targets as underwater corner reflectors, the finite element coupled boundary method can be used to solve the scattered sound field problems in infinite waters with high accuracy.

In order to improve the antiacoustic performance of a corner reflector, where sound waves cannot propagate under vacuum conditions, a vacuum layer is used to act as antiacoustic material, and according to the corner reflector's small concave structural characteristics, elemental coupling of the indirect boundary element method with an underwater hollow cavity corner reflector body scattering acoustic field simulation, we conduct a comparative analysis of the common metal corner reflector acoustic reflectivity characteristics of the law, to explore more effective ways to improve its acoustic reflectivity. Through the pool experiments in the typical conditions of the test, we provide the basis for practical engineering applications of the vacuum cavity underwater corner reflector.

2. Acoustic Scattering Solution for Underwater Targets

The steel surface of a typical underwater corner reflector has acoustic impedance characteristics and excellent sound reflection performance when the water mismatch is large. The reflection coefficient of a 0~20 mm thick elastic steel plate within 0~20 kHz incident sound wave is analysed in Figures 1 and 2, and it can be seen that for the metal plate at a thickness of less than 10 mm, the sound transmission is better, with very obvious elastic characteristics [11, 12], which will cause the coupled vibration of the metal sheet in the water, so that the metal plate will bend with symmetrical vibration [13]; the sound wave has a large elasticity loss during the reflection process, which leads to poor acoustic sound scattering characteristics. When the reflective surface is 10 mm thick, the steel plate antisound coefficient of 0.9 tends to be fully reflective; with the reflective surface increased to a thickness of 20 mm, the antisound coefficient is infinitely close to 1, and the steel plate can be regarded as ideal. The incident acoustic wave and the steel do not produce the acoustic vibration of the coupling effect. Restricted by the density of the steel plate of the corner reflector itself, usually not more than 10 mm thick, when the incident wave frequency is 0~15 kHz, the antisound coefficient of the steel plate composed of the corner reflector is below 0.9, which is in the steel and elasticity critical point, so it is necessary to carry out coupling analysis.

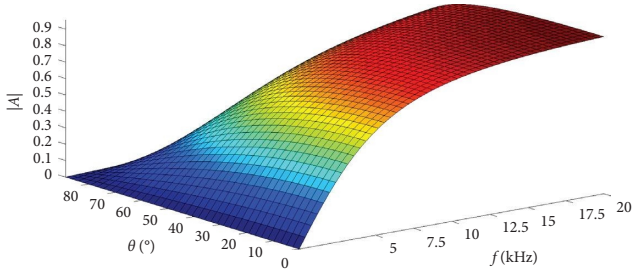

Figure 1: Variation of an elastic metal plate with incident wave angle and frequency.

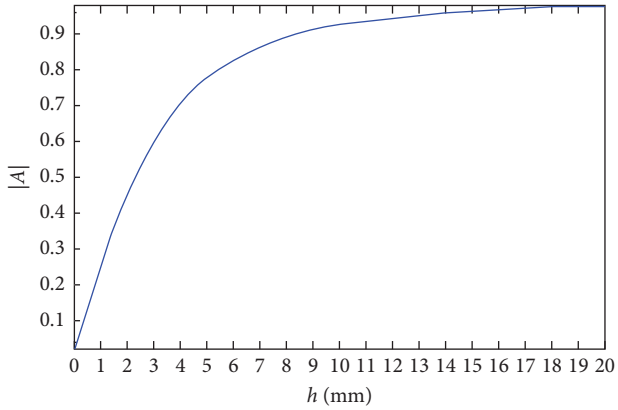

Figure 2: Variation of reflection coefficient with the thickness of metal plate.

2.1. Acoustic Scattering Calculation Method. Let the corner reflector be in an ideal fluid and Q is an arbitrary point on the surface S of the structure, and according to the fluctuation equation and the Helmholtz equation of the scattered acoustic field, the acoustic pressure can be obtained at any field point P in space.

$$p = \int\int_s \left[\mathbf{G}\boldsymbol{\sigma} - \frac{\partial G}{\partial \mathbf{n}}\boldsymbol{\mu}\right] \mathrm{dS}, \tag{1}$$

where $\mathbf{G}$ is the Green's function, $\boldsymbol{\sigma}$ and $\boldsymbol{\mu}$ are the difference in normal pressure gradient and pressure difference on both sides of the surface, respectively, and $\mathbf{n}$ is the outward unit vector on the surface of the structure. Here,

$$\begin{aligned} \boldsymbol{\sigma} &= -j\rho\omega\left(\mathbf{v}_1 - \mathbf{v}_2\right), \\ \boldsymbol{\mu} &= \mathbf{p}_1 - \mathbf{p}_2, \end{aligned} \tag{2}$$

where ρ is the fluid density, ω is the circular frequency, $\mathbf{v}_1$ and $\mathbf{v}_2$ are the normal vibration velocity on both sides of the surface, and $\mathbf{p}_1$ and $\mathbf{p}_2$ are the acoustic pressure on both sides of the surface.

Assuming that the boundary conditions satisfy Neumann and the point P is on the boundary, the relationship between the boundary conditions and the unknown quantities can be expressed as follows:

$$\frac{\partial \mathbf{p}}{\partial \mathbf{n}} = \int\int_s \left[\frac{\partial \mathbf{G}}{\partial \mathbf{n}}\boldsymbol{\sigma} - \frac{\partial G}{\partial \mathbf{n}\partial \mathbf{n}_Q}\boldsymbol{\mu}\right] \mathrm{dS} = -j\rho\omega \mathbf{v}_p, \tag{3}$$

where $\mathbf{v}_p$ xx is the normal vibrational velocity at point P and $\mathbf{n}_Q$ is the outer normal unit vector at point Q.

According to the indirect boundary element theory, after discretising the surface, the fluid pressure load can then be expressed as follows:

$$\mathbf{F}_e^l = -\mathbf{R}_{sf}^e\left(\mathbf{P}_1^e - \mathbf{P}_2^e\right) = -\mathbf{R}_{sf}^e \delta \mathbf{p}^e, \tag{4}$$

where $\mathbf{R}_{sf}^e$ is the fluid-structure coupling matrix, $\mathbf{P}_1^e$ and $\mathbf{P}_2^e$ are the sound pressures at the nodes on both sides of the boundary, and $\delta \mathbf{p}^e$ is the node sound pressure variance.

The finite element equation can then be expressed as follows:

$$\left(\mathbf{K}_s - \omega^2 \mathbf{M}_s\right)\mathbf{U}^e - \mathbf{R}_{sf}^e \delta \mathbf{p}^e = \mathbf{F}_s^e, \tag{5}$$

where $\mathbf{K}_s$ is the structural stiffness matrix, $\mathbf{M}_s$ is the structural mass matrix, $\mathbf{U}^e$ is the node displacement vector, and $\mathbf{F}_s^e$ is the external force matrix on the structural nodes. By the structural vibration, equilibrium conditions can be obtained:

$$\mathbf{F}_a = \mathbf{A}\delta \mathbf{p}^e, \tag{6}$$

where $\mathbf{F}_a$ is the acoustic excitation vector function and $\mathbf{A}$ is the symmetry matrix.

In fluid-solid coupling, the boundary condition is $\mathbf{v}_n = i\omega \mathbf{u}_n$, and the force for the normal motion of the structure is as follows:

$$\mathbf{F}_v = -\rho_s \omega^2 \mathbf{R}_{\mathrm{sf}}^{e\ T} \mathbf{U}^e, \tag{7}$$

where $\mathbf{v}_n$ is the velocity normal to the surface of the boundary element model, $\mathbf{u}_n$ is the displacement normal to the surface of the boundary element model, and ρ_s is the structural density.

Combining equations (6) and (7), the following equation can be derived:

$$\mathbf{F}_a + \mathbf{F}_v = \mathbf{A}\delta \mathbf{p}^e - \rho_s \omega^2 \mathbf{R}_{\mathrm{sf}}^{e\ T} \mathbf{U}^e. \tag{8}$$

Combining equations (5) and (8), the coupled structural finite element and fluid boundary element equations can be obtained as follows:

$$\begin{bmatrix} \mathbf{K}_s - \omega^2 \mathbf{M}_s & -\mathbf{R}_{sf}^e T \\ \rho_s \omega^2 \mathbf{R}_{sf}^e T & \mathbf{A} \end{bmatrix} \begin{bmatrix} \mathbf{U}^e \\ \delta \mathbf{p}^e \end{bmatrix} = \begin{bmatrix} \mathbf{F}_s^e \\ 0 \end{bmatrix}. \tag{9}$$

According to the abovementioned theory, the corner reflector is modelled using the modelling software ANSYS, and the model data are imported into the acoustic analysis software SYSNOISE to analyse its underwater scattered sound field and compare it with the steel single-layer metal plate corner reflector, and the simulation process is shown in Figure 3.

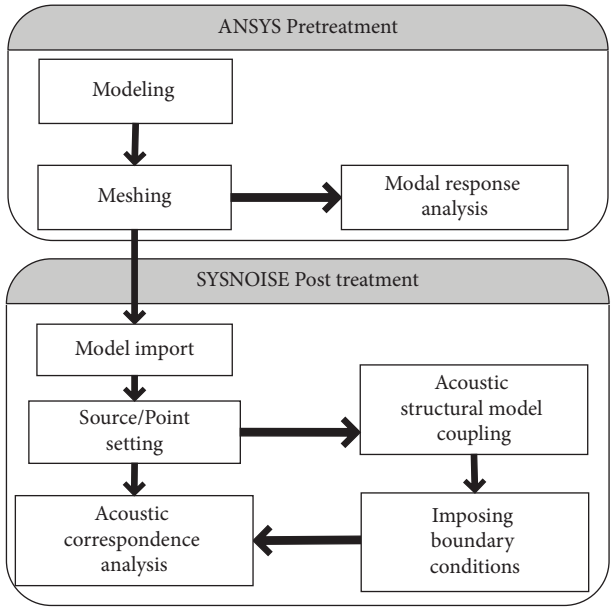

Figure 3: Simulation calculation process.

3. Acoustic Scattering Characterisation Enhancement Method

In order to enhance the acoustic scattering characteristics of underwater corner reflector, according to the principle of acoustic impedance mismatch, the greater the difference between the acoustic impedance characteristics of the acoustic reflecting surface material and water, the better the antiacoustic performance of the corner reflector. Domestic scholars Luo and Xin [14] used the serious mismatch between the characteristic impedance of air and water to design a kind of underwater air-cavity corner reflector, and when they compared with the single-layer metal corner reflector, the air-cavity corner reflector showed good anti-acoustic performance, and the scattering characteristics were similar to those of the steel corner reflector, which is an excellent underwater corner reflector; scholars Yu et al. [15] put forward a kind of underwater corner reflector with a foam sandwich layer, but due to the small acoustic impedance characteristics of the foam layer, it could not significantly improve the acoustic performance of the underwater corner reflector.

Under normal temperature and pressure conditions, the acoustic impedance characteristics of water and air are seriously mismatched, so the air layer can be used as good acoustic material, but it is very difficult to make the air into an independent acoustic layer [16]. Domestic scholars use rubber wrapped in metal to construct the air layer [17], but while the rubber is good at transmitting sound, it cannot achieve a high acoustic coefficient of reflection, and it is complicated to process with a low cost-effectiveness ratio.

Aiming at the abovementioned factors, we compare the acoustic reflection characteristics of the corner reflector with two different designs of a single-layer metal and air cavity. Then, we analyse the improvement of the acoustic reflection ability of the corner reflector due to the vacuum cavity.

3.1. Structural Design of a Vacuum Cavity Corner Reflector. Sound waves cannot propagate in a vacuum environment; when the sound wave incident on the vacuum layer can theoretically be reflected completely, the reflection coefficient is 1, so the vacuum layer can be used as a good antisound material. Because of the inability to achieve an independent vacuum layer, the design of the vacuum cavity utilizes a "sandwich" structure in the metal sheet manufacturing to create a closed cavity outside the installation of the pumping valve, so this metal cavity can be pumped to a near-vacuum state. At this time, the corner of the reflector has two layers of antisound material, the external metal material antisound layer and the internal vacuum antisound layer. A structure with a vacuum cavity for a right angle isosceles triangle with a side length $L = 500$ mm, the upper and lower layers of metal for the steel at a thickness of 2 mm, and the thickness of the internal cavity $H = 10$ mm is shown in Figure 4.

3.2. Comparative Analysis of Acoustic Scattering Characteristics Simulation. Figure 5 shows the schematic diagram of the sound wave incident to the angular reflector, where φ is the angle between the incident sound wave and the plane Oxz, and θ is the angle between the incident sound wave and the axis. We define the incident sound wave as a plane wave, $\theta = 90^\circ$, $\varphi = 0\sim90^\circ$, frequency of 5 kHz, 10 kHz, 15 kHz, with an amplitude of 1 Pa, the sound source from the centre of the target at 100 m, where the field point and the location of the sound source are the same. To meet the conditions of the far-field and send/receive the joint position, the flow medium for water is set at room temperature and the pressure to a density of 1,000 kg/m^3, the sound wave propagation velocity of 1,500 m/s in the water, and the acoustic wave angle of incidence is $\varphi = 0^\circ\sim90^\circ$, every 5° for a calculation.

The metal material of the reflector is defined as steel, with modulus of elasticity $E = 2.1e11$ Pa, Poisson's ratio of 0.3, density of 7800 kg/m^3, and side length $L = 500$ mm. The thickness of the reflecting surface of the single-layer metal corner reflector is $H = 10$ mm; the thickness of the metal reflecting surface of the vacuum cavity corner reflector is $H = 2$ mm, and that of the vacuum cavity is 10 mm, with vacuum conditions inside the cavity. Under different incident frequencies and incident angles, the simulation results of the target strength (TS) curves of the corner reflector are shown in Figure 6.

As can be seen from Figure 6, the characteristic curve of the target intensity value of the single-layer steel corner reflector with the frequency change of the incident wave is symmetric along $\varphi = 45^\circ$; the maximum target intensity value is achieved when the incident acoustic wave is 15 kHz, which shows obvious frequency characteristics; the scattering width is small, which can only maintain a high target intensity value in a small acoustic wave incident angle.

True cavity three-sided angular reflector target intensity value with the incident wave frequency with the horizontal angle of incidence change law curve along the $\varphi = 45^\circ$ symmetry; frequency characteristics are obvious in the incident acoustic wave for 15 kHz to achieve the maximum target intensity value, the incident acoustic wave frequency is reduced, the target intensity value of the attenuation of the faster, scattering width range is large, and the angle of incidence within the higher target intensity value, the return of the stability of the wave is strong.

Comparative analysis shows that the frequency characteristics of the corner reflector are obvious and compared with the single-layer steel three-sided corner reflector, the vacuum cavity corner reflector has a larger target intensity value and a wider range of scattering width, which can achieve more excellent acoustic scattering characteristics under the same dimensions and has an improved effect on the acoustic scattering characteristics.

The air cavity corner reflector has strong frequency characteristics [14], and when comparing and analysing with the true air cavity corner reflector, the rest of the parameters of the incident source remain unchanged; the incident wave frequency is 15 kHz, the rest of the simulation parameters remain unchanged, and the results are shown in Figure 7.

The two types of corner reflectors have the same trend of target intensity change, and the comparative analysis shows that the target intensity curve of the vacuum cavity corner reflector is smooth, and there are high target intensity values in 0–90° with large scattering width and good decoupling effects, proving the vacuum cavity corner reflector has better acoustic scattering performance.

4. Experimental Verification

In order to verify the ability of the vacuum layer to improve the acoustic scattering characteristics of the angular reflector, the experimental prototype of the vacuum cavity three-sided angular reflector processing is shown in Figure 8. The vacuum cavity corner reflector consists of three independent metal cavities perpendicular to each other. The cavity is connected to a one-way pumping ball valve, which is connected to the air pressure gauge. The air compressor is used to pump out the internal air of the cavity to 0.06 Pa, close to the state of a vacuum. Compared with the steel three-sided angle reflector, the hollow cavity angle reflector with a single cavity mass of 3.9 kg and an overall mass of 11.7 kg, not counting the cavity bracket, is much smaller than the single layer of the steel three-sided angle reflector at 30 kg, so it has a better engineering practicality.

The parameters are shown for a 6 m ∗ 4 m ∗ 4 m reverberation pool, equipped with two skids as fixed devices. The fixtures are used to suspend the experimental equipment in the reverberation pool, and the distance between the experimental equipment is adjusted by means of the skids.

In the test device layout shown in Figure 9, the corner reflector with a cable connection is suspended in the water, ignoring the influence of the thin rope on the sound scattering; the standard hydrophone and transmitting transducer external PVC tube is suspended into the water to

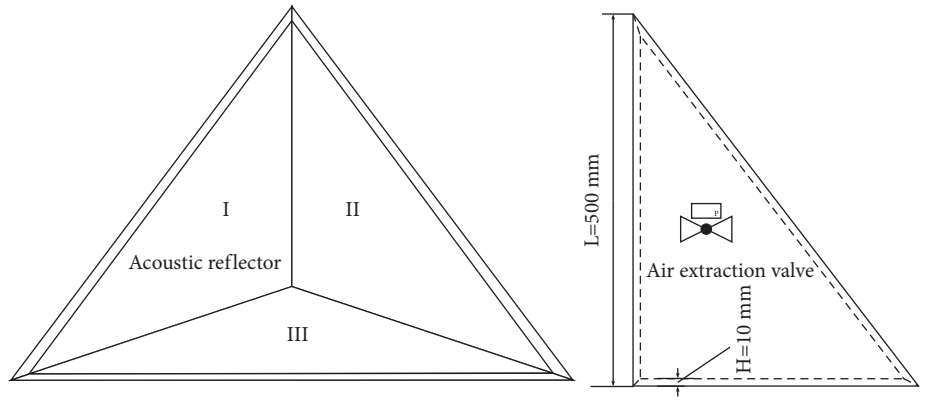

Figure 4: Design drawing of a vacuum cavity corner reflector.

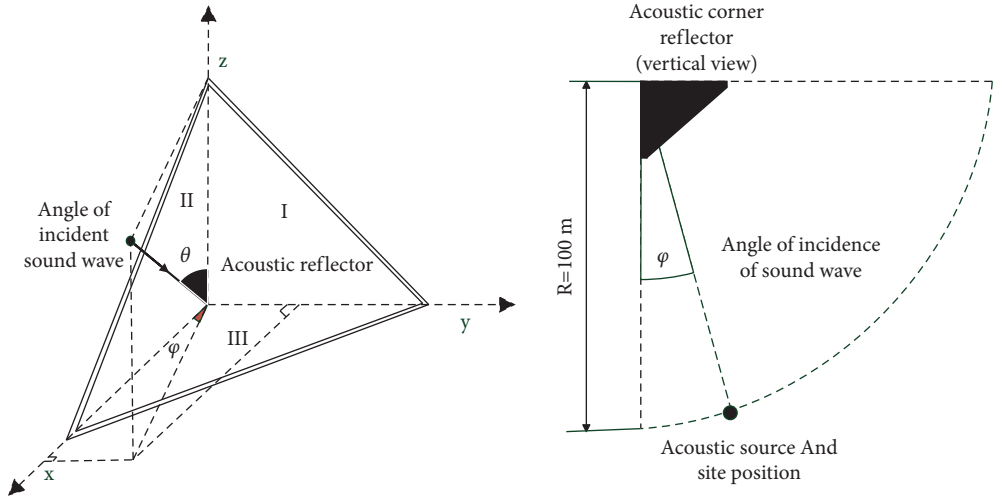

Figure 5: Analysis method for acoustic scattering characteristics of corner reflectors.

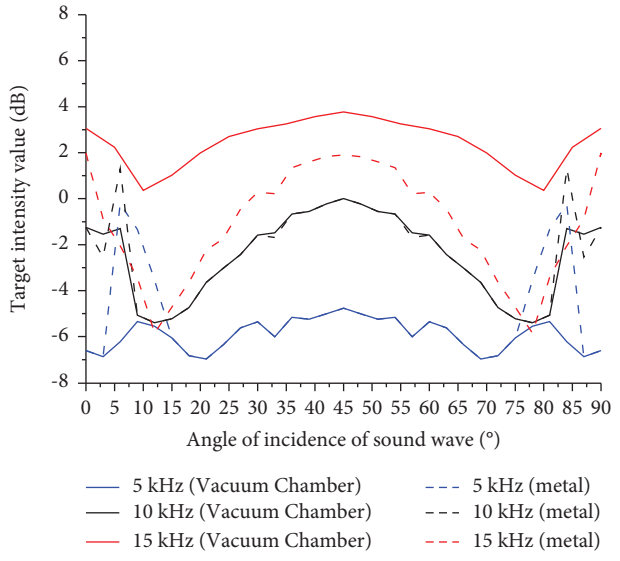

Figure 6: Comparison chart of the target intensity value frequency curve between vacuum chamber and single layer metal corner reflector.

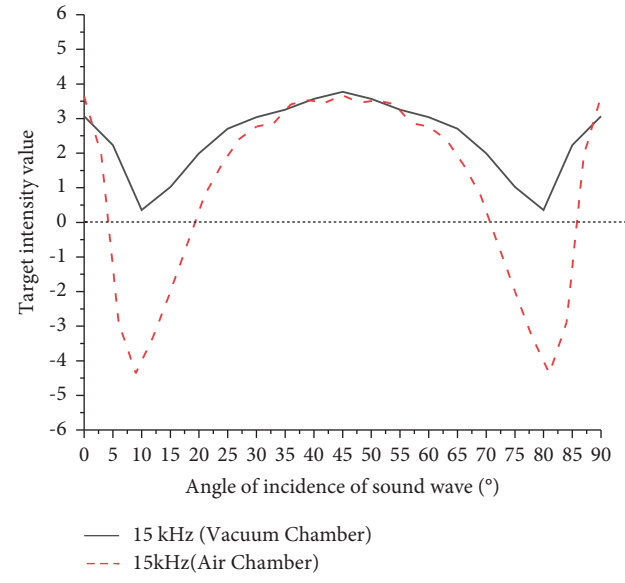

Figure 7: Comparison chart of the target intensity value frequency curves for vacuum chamber and air chamber reflectors at 15kHz.

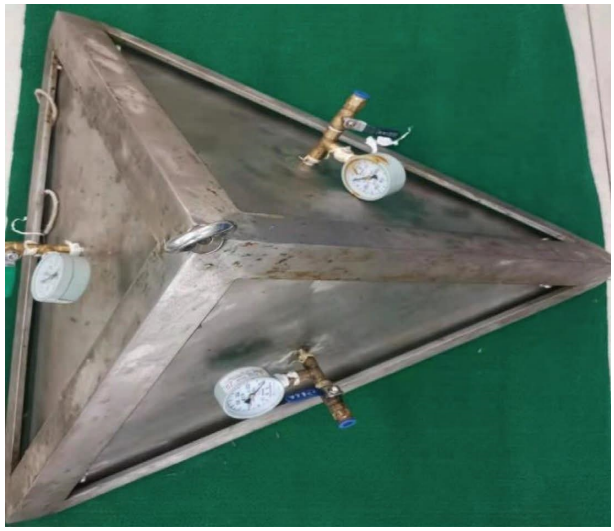

Figure 8: A vacuum layer corner reflector.

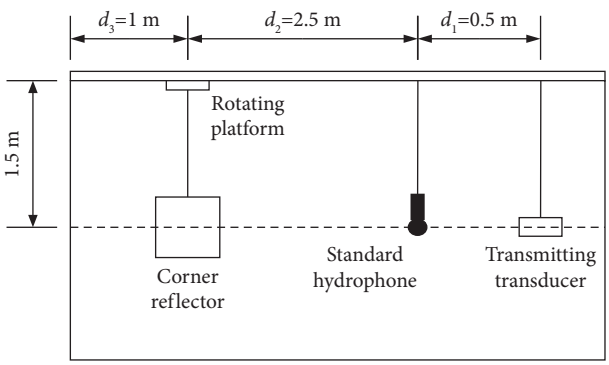

Figure 9: Layout of experimental instruments.

ensure that the acoustic centre of the three test equipment parts are at the same depth. The direction of the transmitting transducer emitting sound waves is directly opposite from the acoustic centre of the angular reflector to ensure the accuracy of the angle of incidence of the sound source. The test equipment pool layout is shown in Figure 10, where the angle of incidence of the sound source is 0°, and the sound wave is vertically incident on the corner reflector of the reflective surface.

The side length of the corner reflector was 0.5 m. Based on the equation L^2/λ, when the incident acoustic source was 15 kHz, the corner reflector was 2.5 m away from the standard hydrophone and 3 m away from the transmitting transducer, which satisfied the far-field conditions. The incident sound waves were continuous wave pulse signals with a pulse cycle of 2 s, a pulse width of 1 ms, and a frequency of 15 kHz. The scattering target intensity was stabilized by no less than ten waves of a narrow pulse width passed within a unit pulse cycle. In this way, the reverberation waves generated by incident pulse signals exerted the minimum effect on the target reflected waves. When the acoustic centers remained unchanged, data were collected at every 5° rotation of the corner reflector. This was intended to measure the influence of angle variation on the

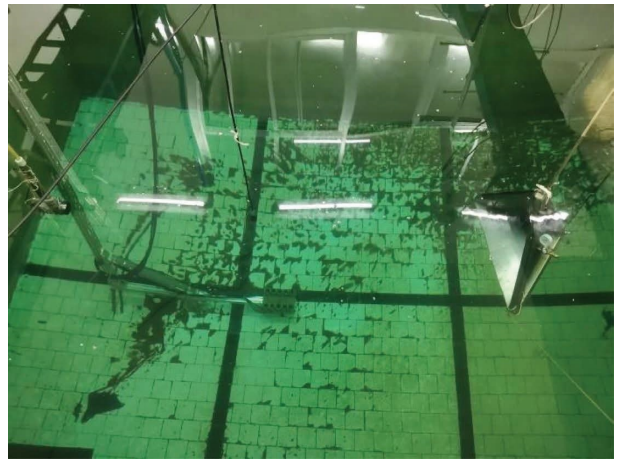

Figure 10: Layout of experimental instruments in the water tank.

target intensity value of the corner reflector. The hydrophone was connected to the oscilloscope. The target intensity echo variation was observed on the oscilloscope, then recorded and analysed.

The hydrophone converted acoustic signals into electrical signals and then displayed them as voltage. The target intensity value is calculated by the following equation:

$$\mathrm{TS} = 20\lg\frac{U_b}{U_d} + 20\lg\frac{d_2}{d_1} + 20\lg\left(d_1 + d_2\right), \tag{10}$$

where d_1 is the distance from the transmitting transducer to the standard hydrophone; d_2 is the distance from the hydrophone to the target corner reflector; U_b stands for the voltage of the echo signals from the corner reflector; and U_d is the voltage of the direct waves. Among them, d_1 and d_2 have been determined in Figure 9, while U_b and U_d are read from the oscilloscope.

In the case of a vacuum cavity, the internal cavity is pumped to make the air pressure inside the cavity as close to a vacuum as possible. Different types of corner reflectors are suspended in the reverberation pool by cables, the corner reflectors are rotated, and measurements are taken once every 5°, the target intensity values change with the incident angle, as shown in Figure 11.

As can be seen from Figure 11, the simulation results of the target intensity of the corner reflector of the vacuum cavity in the real measurement of the reverberant pool are basically the same as the experimental results, thus verifying the correctness of the calculation results and also proving the contribution of the vacuum cavity to increase the echo intensity of the corner reflector.

The target intensity value of the corner reflector of the vacuum cavity under the experimental conditions is about 0.6 dB higher than that of the simulation calculation, and this error is caused by the fact that the reverberant pool is small, and the wall reverberation cannot be completely avoided, which results in the superposition of the reverberant wave and the scattered wave of the corner reflector of the vacuum cavity. Compared with the simulation results, the characteristic curve of the target intensity test value of

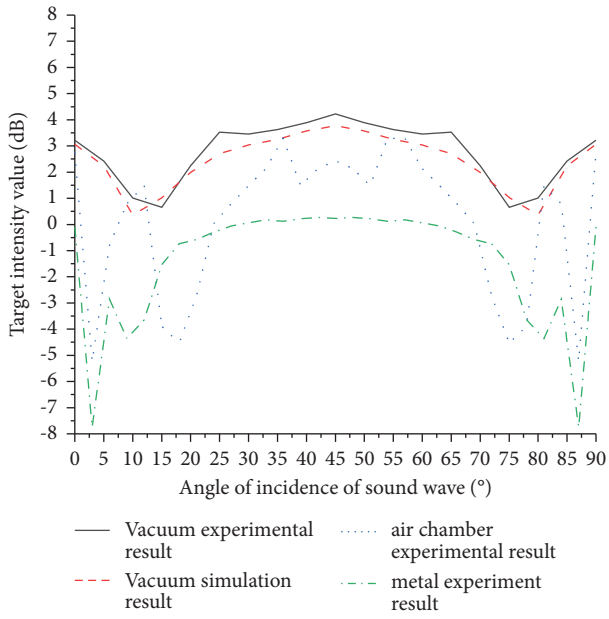

Figure 11: Comparison of experimental results of a vacuum cavity trihedral corner reflector.

the vacuum cavity three-sided corner reflector is sharper, which is due to the fact that in the actual test, the corner reflector in the underwater rotation of the human error is larger, and the acoustic wave incidence angle sampling points are fewer.

In summary, it can be seen that, due to the serious mismatch of acoustic impedance characteristics between the cavity and the water medium layer, the acoustic scattering characteristics of the vacuum cavity corner reflector are better than those of the single-layer metal and air cavity three-face corner reflector under the actual experimental conditions, and the acoustic scattering characteristics of the three-face corner reflector can be greatly improved, so the reasonableness of the design of the vacuum cavity corner reflector has been proven.

5. Conclusion

According to the characteristics of the acoustic properties of the serious mismatch of air and water impedance, this paper offers a design for a true air cavity three-sided corner reflector. Comparative analyses of acoustic scattering characteristics are carried out with single-layer steel and air-cavity corner reflectors, and the simulation results are experimentally verified in a typical pool. The results show that the hollow cavity corner reflector has good antiacoustic performance, no obvious frequency characteristics, a large scattering width, and good decoupling effect and at the same time, the overall weight is reduced by about 20 kg, which is of strong value for engineering applications, because the hollow cavity can be used as an ideal method to improve the acoustic scattering characteristics of the underwater corner reflector.

Due to time limitations, this paper studies and analyses only the acoustic scattering characteristics of a typical three-surface vacuum cavity corner reflector and leaves the collapse problem of a vacuum cavity under deep water conditions for future studies. Further research is needed to determine the acoustic scattering characteristics of the multigrid reflector composed of multiple corner reflectors as well as the rationality of the structural design.

Data Availability

The data that support the findings of this study are available from the corresponding author upon reasonable request.

Conflicts of Interest

The authors declare that they have no conflicts of interest.

References

[1] C. Shuai, G. C. Liao, Y. X. Zhang, W. Ma, and H. Wen, "Simulation on effect of manufacturing deviation of inflatable corner reflector on monostatic RCS," *Journal of Nanjing University of Science and Technology*, vol. 43, no. 2, pp. 193–198, 2019.

[2] Z. Y. Zhang, J. C. Lee, W. Yang et al., "Percutaneous ablation of the tumor feeding artery for hypervascular hepatocellular carcinoma before tumor ablation," *International Journal of Hyperthermia: The Official Journal of European Society for Hyperthermic Oncology, North American Hyperthermia Group*, vol. 35, no. 1, pp. 133–139, 2018.

[3] H. C. Zhao, "Design of an X-band omnidirectional radar angular reflector array," *Journal of the Hebei Academy of Sciences*, vol. 36, no. 1, pp. 26–29, 2019.

[4] T. Gitiesr and C. A. Balanis, "Dihedral corner reflectors backscatter using higher order reflections and diffractions," *IEEE Transactions on Antennas and Propagation*, vol. 35, no. 11, pp. 1235–1247, 1987.

[5] W. J. Chen, "Study on the acoustic backscattering characteristics of underwater corner reflector," *Journal of Information and Computational Science*, vol. 12, no. 1, pp. 1–7, 2015.

[6] W. L. Tang, J. Fan, and Z. C. Ma, *Acoustic Scattering of Underwater target*, Science Press, Beijing, China, 2018.

[7] W. Luo, H. He, and C. Xin, "A method of cheating and countering moving mines using corner reflectors," *Command Control and Simulation*, vol. 38, no. 05, pp. 112–115, 2016.

[8] W. E. I. Ke-nan, L. I. Wei, M. Lei, and Y.-B. Chai, "The low-frequency acoustic scattering characteristics study on underwater targets by the coupled boundary element method," *Ship Science And Technology*, vol. 10, no. 36, 2014.

[9] A. M. Shaaban, C. Anitescu, E. Atroshchenko, and T. Rabczuk, "3D isogeometric boundary element analysis and structural shape optimization for Helmholtz acoustic scattering problems," *Computer Methods in Applied Mechanics and Engineering*, vol. 384, Article ID 113950, 2021.

[10] X. Chen, Y. Luo, and A. H. Li, "Acoustic scattering characteristics of underwater elastic corner reflectors," *Acta Armamentarii*, vol. 39, no. 11, pp. 2236–2242, 2018.

[11] H. W. Hu, Z. W. Wang, and Y. M. Xu, "A study on the isogeometric finite element-boundary element method for the stochastic analysis of structural acoustic coupling," *Journal of Vibration and Shock*, vol. 41, no. 12, pp. 159–167, 2022.

[12] X.-F. Zhao, C. Hai-chao, and R. Dong, "Simulation experiment of underwater elastic plate scattering sound field with

lamb wave," *Digital Ocean & Underwater Warfare*, vol. 2, no. 3, pp. 31–33, 2019.

[13] Y. Luo, J.-Y. Wang, and X. Tao-tao, "A foam interlayer method for improving on the acoustic reflection capability of underwater corner reflector," *Acta Armamentarii*, vol. 41, no. 10, pp. 2081–2087, 2020.

[14] Y. Luo and C. Xin, "Acoustic Scattering characteristics of underwater air-filled cavity corner reflector," *Acta Armamentarii*, vol. 40, no. 10, pp. 29–35, 2019.

[15] M. Yu, J.-X. Zhou, and Y.-O. Zhang, "Application of acoustic metasurface in reducing sound scattering of a plate," *Journal of Huazhong University of Science and Technology (Natural Science Edition)*, vol. 47, no. 8, pp. 76–80, 2019.

[16] C. Lei, Y. Ma, and X. Lin, "Study on a new kind of marine acoustic reflecting material," *Development and Application of Materials*, vol. 19, no. 2, pp. 10–12, 2004.

[17] J. Fan, X. Zhao, and X. Han, "Preparation and properties of a new underwater acoustically transparent rubber," *China Rubber Industry*, vol. 61, no. 03, pp. 133–137, 2014.